Lithosphere structures of Alaska revealed by ambient-noise adjoint tomography

Tianshi Liu[1], Kai Wang[2], Ping Tong[3], Carl Tape[4] and Qinya Liu[1]

(1) University of Toronto, Toronto, ON, Canada, (2) Macquarie University, Sydney, NSW, Australia,
(3) Nanyang Technological University, Singapore, Singapore, (4) University of Alaska Fairbanks, Fairbanks, AK, USA.

Abstract

Alaska, located at the northernmost of the North American Cordillera, is one of the most tectonically active regions in North America. Its unique geological structure is a record of a complex tectonic history, which includes a series of events of collision and deformation, and the ongoing subduction in the south. This study aims to image the lithosphere structures beneath Alaska using seismic tomography.

The ambient-noise tomography technique (Shapiro & Campillo, 2004) is widely used to take advantage of dense seismic arrays to map the subsurface structures. However, most traditional ambient-noise tomography studies are often based on ray approximation and two-step inversion where phase velocity maps at different frequencies are obtained and inverted. The adjoint tomography method, sometimes also referred to as full-waveform inversion (Tromp et al 2005, Liu & Gu 2012) was proposed to address this limitation by using the numerical solver directly as the forward operator and applying numerical optimization algorithms to solve the nonlinear inverse problem and update the velocity model iteratively. In order to produce an accurate and high-resolution tomographic image, we combine the ambient-noise tomography technique and the adjoint tomography method to map the shear-velocity structures in the lithosphere of Alaska.

Long-period continuous time-series data recorded between June 2014 and September 2019 by 436 seismic stations in Alaska are downloaded and preprocessed, and cross-correlations are computed and stacked to extract the vertical-component Rayleigh-wave empirical Green's functions (EGFs). Frequency-dependent travel-time misfits between the EGFs and the simulated Green's functions (SGFs) are measured at 12-25s, 18-36s and 25-50s bands, and are minimized to iteratively update the velocity model. Our final model extends from the surface down to 70 km beneath the entire Alaska region. Highlighted features in the model include: (1) low-velocity anomalies in the upper-crust matching with sedimentary basins; (2) a high-velocity subducted Slab along the southern shore and a low-velocity mantle wedge south of the Denali Fault; (3) a high-velocity cratonic block in the north.

Geological settings
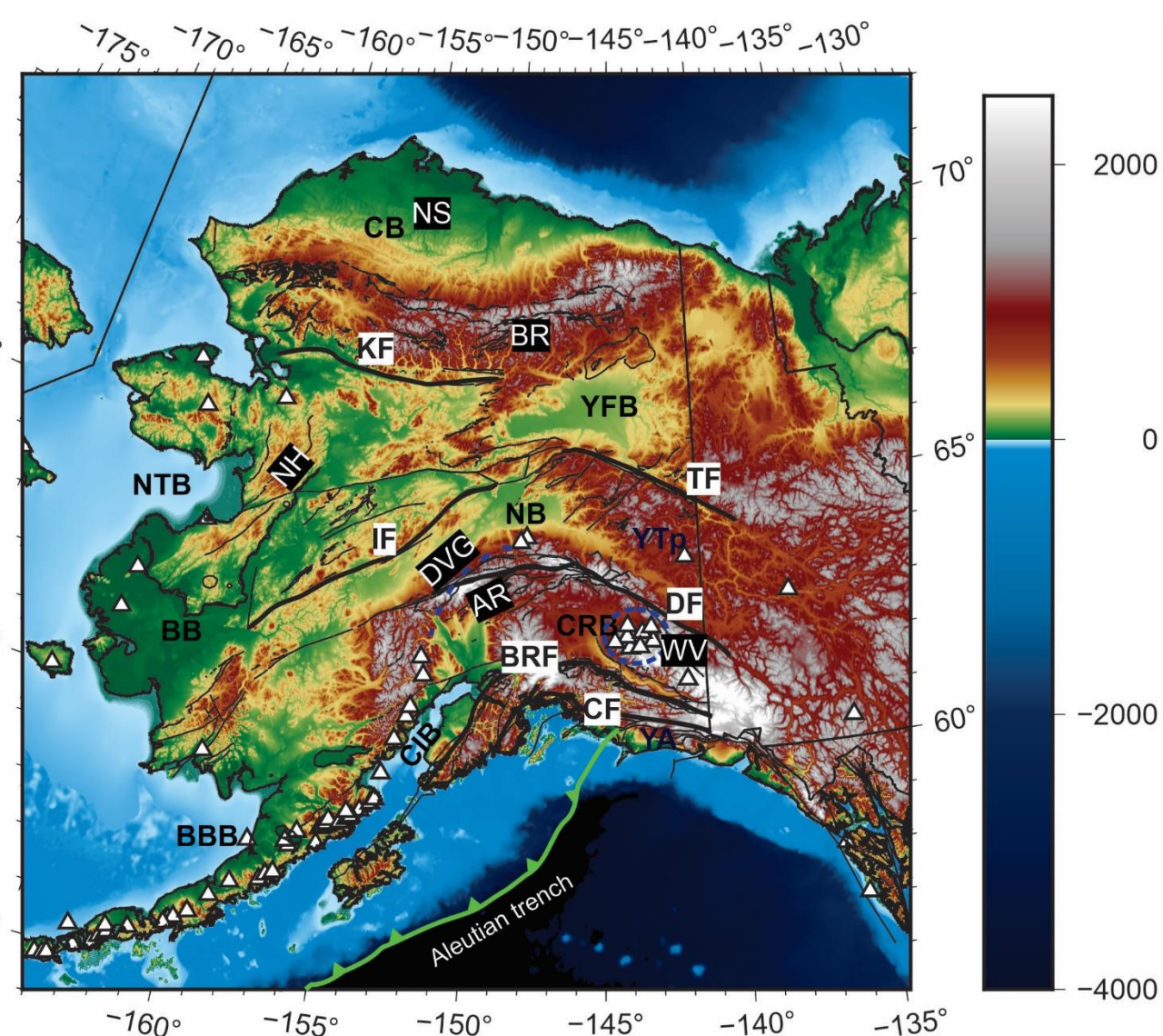
Major geologic structures in Alaska. White triangles represent volcanoes. Black texts with no backgrounds mark major sedimentary basins. Black texts with white backgrounds denote major faults. White texts with black backgrounds are selected geologic features, e.g., volcanic fields, mountains, etc.

Seismic stations in Alaska
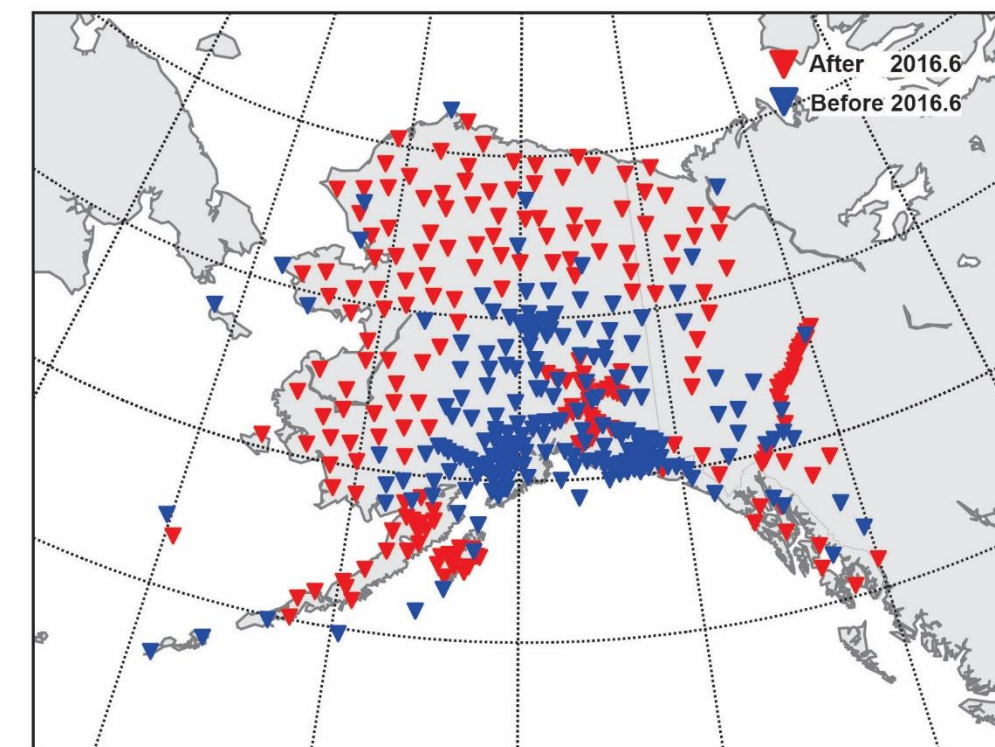
Distributions of long-period seismic stations in Alaska. Coverage in northern & western Alaska is significantly improved due to deployment of USArray (IRIS DMC, 2010).

Workflow of ambient-noise adjoint tomography
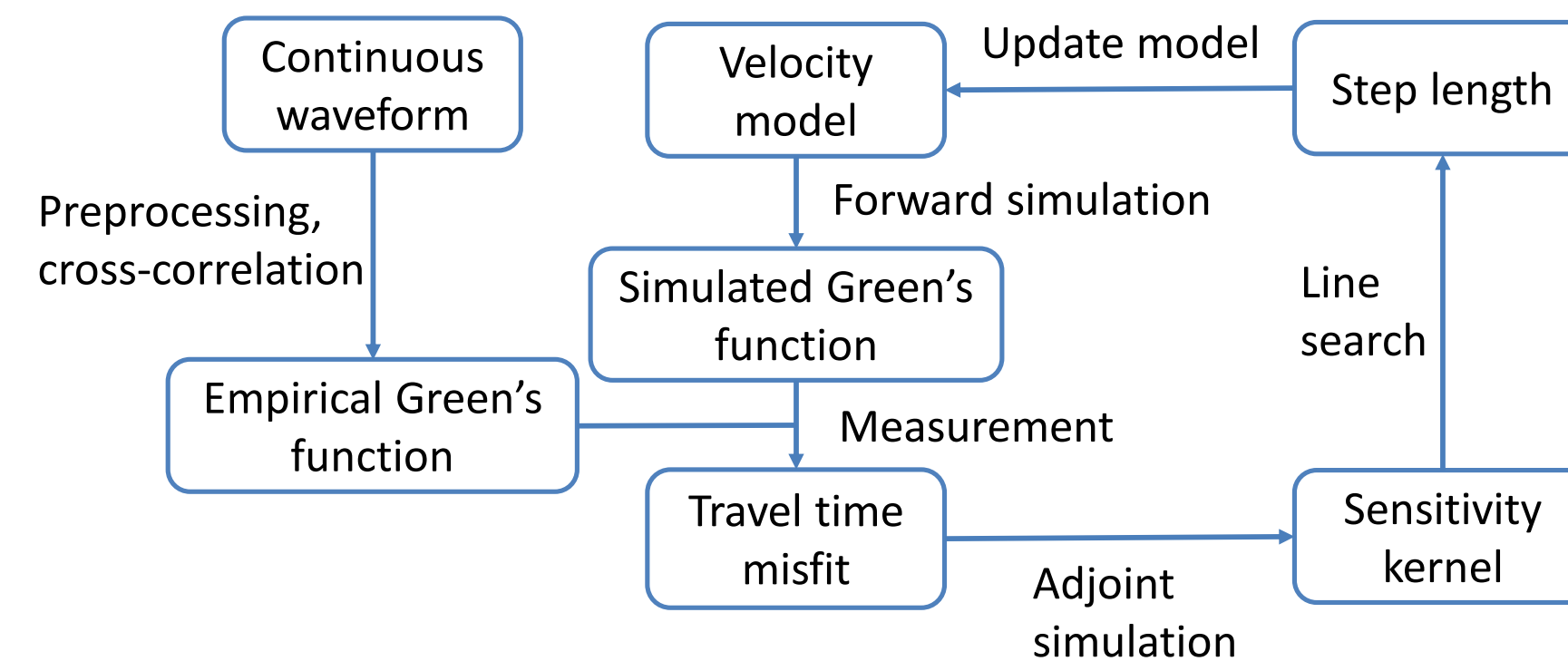

Inversion details:

- Vertical-component continuous time-series data 2014.6 – 2019.9 (63 months)
- 436 stations, 48096 station pairs with > 1-year overlap
- Initial model: S40rts (Ritsema et al., 2011) + Crust 1.0 (Laske et al., 2013)
- Numerical simulation: SPECFEM3D (Komatitsch & Tromp, 1999)
- Three period bands: 25-50s, 18-36s, 12-25s
- Hierarchical strategy to prevent cycle-skipping
  - 1st – 6th iteration: 25-50s only
  - 7th – 11th iteration: 25-50s + 18-36s
  - 12th – 24th iteration: all three period bands
- Kernel smoothing: horizontal 30km, vertical 10km
- Model update: L-BFGS + line search

Mesh for numerical simulation
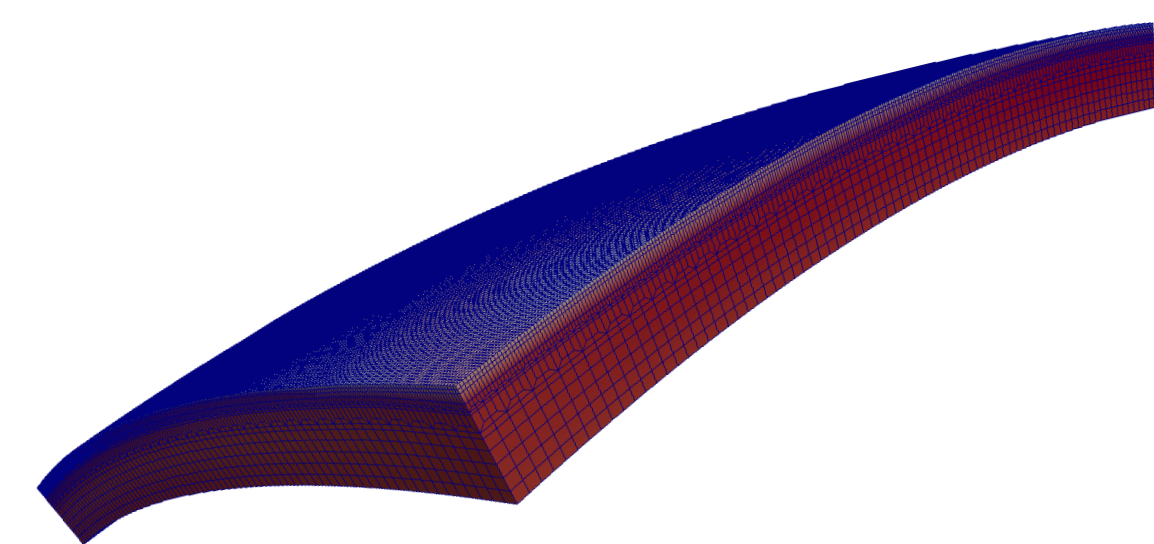
- ✓ 3D velocity model
- ✓ Internal & surface topography
- ✓ Sphereical curvature and ellipticity
- ✓ Mesh doubling in the lower-crust and beneath Moho

Misfit reduction and time-shift histograms
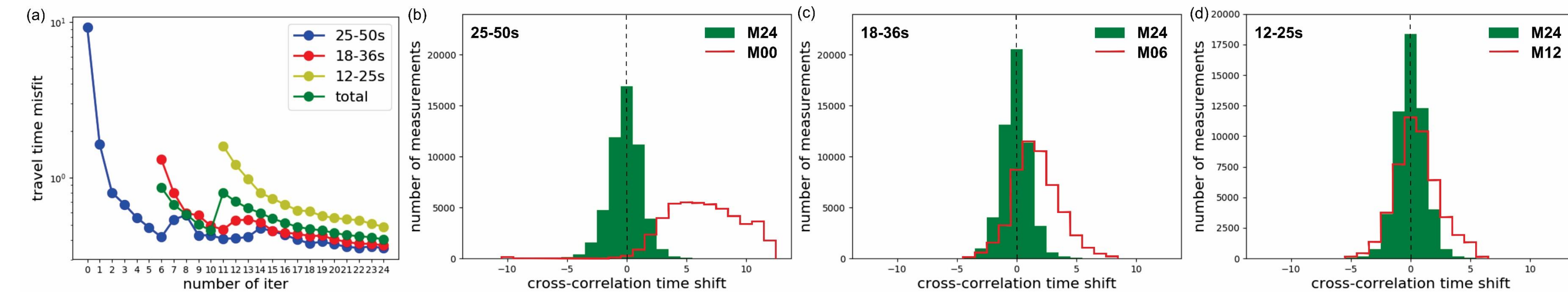
(a) Misfit decrease with iterations, for each individual period band and total. (b) – (d) Histograms of the cross-correlation time-shifts between the SGFs and the EGFs, when each period is first included (red lines) and after 24 iterations (green blocks), for the three period bands. The vertical dashed lines mark the position of zero time-shift. The positive biases when each period band is first included indicate that the initial model is faster than the real structure. The time-shifts are centered at zero for the final model, indicating the biases are corrected.

Result: Shear-velocity model
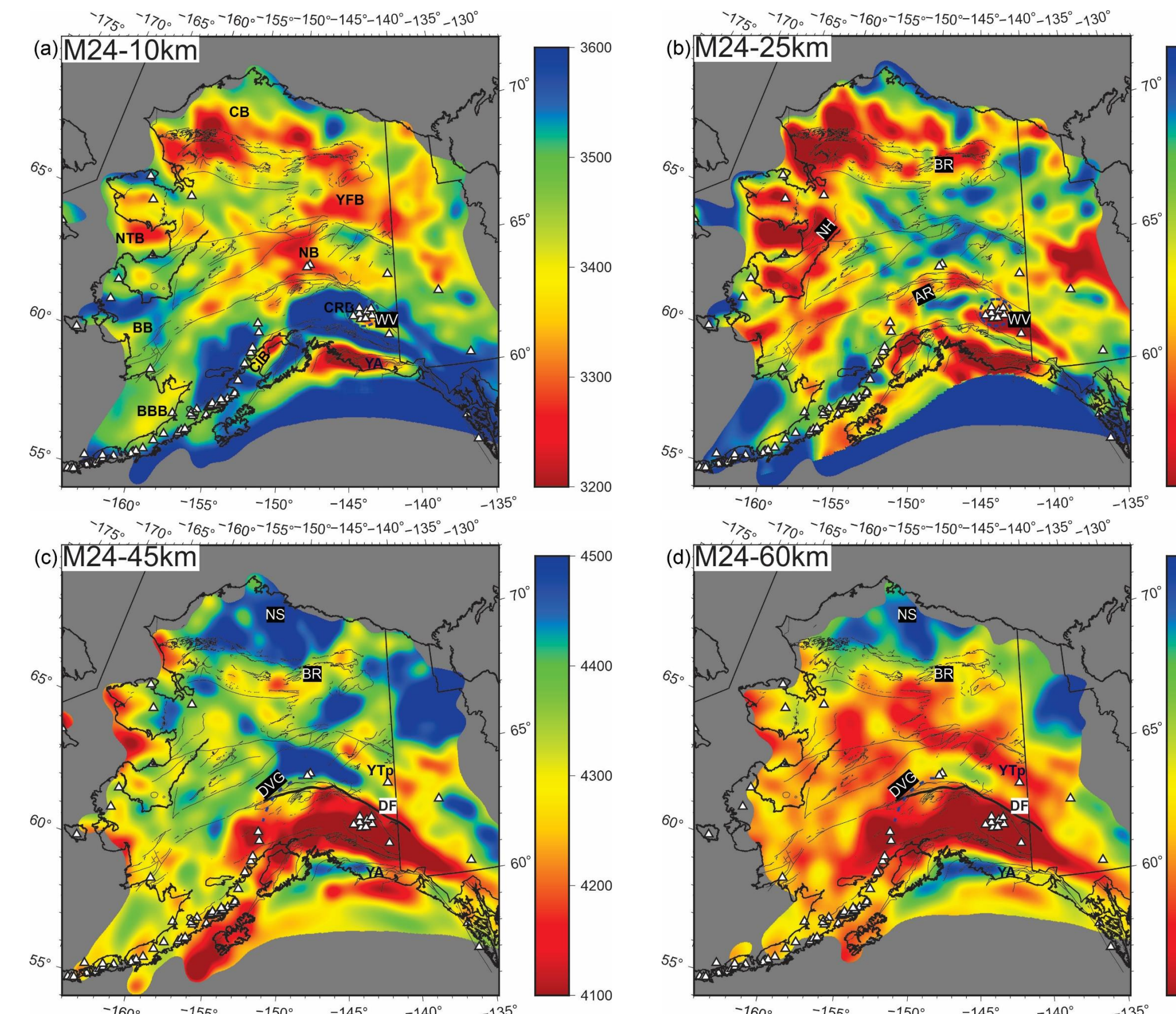
10km depth:
- Low velocity related to sedimentary basins
- Yakutat Terrane (YT) and the Wrangell Volcanic Fields (WV) are characterized by low velocity

25km depth:
- Low velocity beneath the Brooks Range (BR) and the Alaska Range (AR)
- Low velocity at Wrangell Volcanic Fields, potentially due to magmatic activities
- High velocity in the interior area between the Brooks Range and the Alaska Range possibly due to crustal thinning

45km & 60km depth:
- Low velocity south of the Denali Fault (DF), related to mantle wedge
- Low velocity discontinues at the Denali Volcanic Gap (DVG)
- High velocity further south immediately onshore, possibly the subducted slab
- Relatively low velocity beneath the Brooks Range and the parautochthonous Yukon-Tenana Terrane (YTp).
- High velocity at the North Slope (NS), representing the cratonic block.

References

Shapiro, N. M. & Campillo, M., 2004. Emergence of broadband Rayleigh waves from correlations of the ambient seismic noise, *Geophys. Res. Lett.*, **31(7)**, 8–11.

Liu, Q. & Gu, Y. J., 2012. Seismic imaging: From classical to adjoint tomography, *Tectonophysics*, **566-567**, 31–66.

IRIS DMC (2010). Data services products: EARS EarthScope automated receiver survey.

Komatitsch, D. & Tromp, J., 1999. Introduction to the spectral element method for three-dimensional seismic wave propagation, *Geophys. J. Int.*, **139(3)**, 806–822..

Ritsema, J., Deuss, A., Van Heijst, H. J., & Woodhouse, J. H., 2011. S40RTS: A degree-40 shear-velocity model for the mantle from new Rayleigh wave dispersion, teleseismic traveltime and normal-mode splitting function measurements, *Geophys. J. Int.*, **184(3)**, 1223–1236.

Laske, G., Masters, G., Ma, Z., Pasyanos, M. E., & Livermore, L., 2013. Update on CRUST1.0 : A 1-degree Global Model of Earth's Crust, *Geophys. Res. Abstracts*, **15**, EGU2013–2658.